

The InSb Auger recombination coefficient derived from the IR-FIR dynamical plasma reflectivity

This article has been downloaded from IOPscience. Please scroll down to see the full text article.

2001 J. Phys.: Condens. Matter 13 7363

(<http://iopscience.iop.org/0953-8984/13/33/316>)

View [the table of contents for this issue](#), or go to the [journal homepage](#) for more

Download details:

IP Address: 171.66.16.238

The article was downloaded on 17/05/2010 at 04:32

Please note that [terms and conditions apply](#).

The InSb Auger recombination coefficient derived from the IR–FIR dynamical plasma reflectivity

S Marchetti, M Martinelli and R Simili

IFAM–CNR, Area della ricerca del CNR, Via G Moruzzi 1, 56124 Italy

Received 18 May 2001, in final form 4 July 2001

Published 2 August 2001

Online at stacks.iop.org/JPhysCM/13/7363

Abstract

In order to reproduce the transient IR–FIR reflectivity and transmission due to an intense photo-plasma generated by a fast laser pulse at a frequency above the band gap, we have used a dynamical model of plasma evolution. In this way we have derived both the ‘quadratic’ and ‘cubed’ coefficients of the Auger recombination in indium antimonide, by analysing the transient reflectivity at 10.6 μ and 119 μ induced by a fast Nd pulse. In particular we have derived a cubic coefficient of about $7 \pm 3 \times 10^{-26} \text{ cm}^6 \text{ s}^{-1}$, a result larger than those derived in previous experimental works but quite in agreement with the theory.

1. Introduction

The Auger recombination (AR) is an intrinsic process that fixes a fundamental limit to the radiative recombination in any optoelectronic device and determines its time response. In the AR process a hole–electron couple recombines and the resulting energy is transferred to a third carrier, and the intensity of this process depends on the band gap and band contour, being faster if the band gap is smaller.

The AR process can follow different channels that can be summarized in two processes: γ_{ehh} and γ_{eeh} with a hole and electron as the third body respectively. In dense neutral plasma with density N for both holes and electrons, the AR process has a cubed dependence on N as $dN/dt = -(\gamma_{ehh} + \gamma_{eeh})N^3 = \gamma_3 N^3$ [1]. [1] calculated $\gamma_3 \sim 3 \times 10^{-26} \text{ cm}^6 \text{ s}^{-1}$ for intrinsic InSb.

A way to measure the AR is to analyse the temporal dynamics of a plasma induced by a fast light pulse at a frequency above the band gap [1–4], typically a Nd laser, and to observe the transient transmission or transient reflectivity of a laser light at frequency under the band gap, typically a CO₂ laser.

In [5] some calculations have been reported and compared to the experimental recombination times observed in fast photodiodes. This work demonstrates that $\gamma_{ehh} \sim \gamma_{eeh} \sim 0.5\gamma_3$, and that, in heavily doped photodiodes, the relaxation time is an AR process depending on the doping concentration as $\tau^{-1} \sim 0.5\gamma_3 N_d^2$ where N_d is the dopant concentration. From the data of [5] we can derive that γ_3 is in the $1 \times 10^{-25} \text{ cm}^6 \text{ s}^{-1}$ range. This

value agrees with the theoretical calculation in [3], where also an experimental investigation has been performed to measure a γ_3 value from the transient reflectivity and transmission at 10.6μ , induced by a long pulse Nd laser and observing that γ_3 was changing from 2×10^{-25} to $1.5 \times 10^{-26} \text{ cm}^6 \text{ s}^{-1}$ by increasing the plasma density. A similar experiment has been performed in [2] by using a ruby laser, and obtaining $\gamma_3 = 3 \times 10^{-27} \text{ cm}^6 \text{ s}^{-1}$. Another γ_3 theoretical estimation can be derived from [6], where the recombination rate is calculated versus the neutral plasma density in InSb, showing a cubic dependence with $\gamma_3 \sim 2.5 \times 10^{-26} \text{ cm}^6 \text{ s}^{-1}$.

[2] and [3] derived an experimental γ_3 AR coefficient smaller than expected and they attributed this result to the fact that the plasma densities were so large as to produce a band modification (Burnstein effect). With this assumption both works obtained a better fit by posing $\gamma_3 \sim 0$ and considering only the ‘quadratic process, $dN/dt = -\gamma_2 N^2$. In this approach they have obtained $\gamma_2 = 7.5 \times 10^{-9} \text{ cm}^3 \text{ s}^{-1}$. The same approach and the same γ_2 value was used in [1] to fit the time relaxation of a transient transmission induced by a ps Nd laser in an InSb thin film, for frequencies a little above the band gap. With the same approach in [4] the measurements were fitted with $\gamma_2 = 1.5 \times 10^{-9} \text{ cm}^3 \text{ s}^{-1}$. This is a surprisingly low value, because, by expanding the AR recombination process for $N \gg N_i$ we have a term $dN/dt = -3\gamma_3 N_i N^2$, so that for dense plasmas we expect $\gamma_2 > 3\gamma_3 N_i$, taking into account that the ‘quadratic’ recombination channel contains also the radiative process. But from [5] and an $N_i = 1.6 \times 10^{16} \text{ cm}^{-3}$ InSb intrinsic concentration at room temperature, the foreseeable value was $\gamma_2 > 5 \times 10^{-9} \text{ cm}^3 \text{ s}^{-1}$, in good agreement with [1] and [3].

In [7] the InSb recombination rate has been derived from pump–probe transmission of infrared FEL ps radiation. The authors interpreted their data with a ‘cubic’ term $\gamma_3 = 1 \times 10^{-26} \text{ cm}^6 \text{ s}^{-1}$, but their data can be also fitted with a ‘quadratic’ $\gamma_2 \sim 6 \times 10^{-9} \text{ cm}^3 \text{ s}^{-1}$.

The results of [1–4] and [7] bring us to the conclusion that, at high plasma densities, the recombination process could be dominated by the ‘quadratic’ dependence, and that the standard ‘cubic’ process can be neglected. Moreover many of them derived their results in quite an indirect way from a simplified model of plasma dynamics, so we could conclude that the question needs further analysis.

An accurate model has been described in [8] and applied in [8–10], relating the space–time dependent plasma density $N(x, t)$ to the observed transmission and reflection of light with frequency under the band gap. In this work we have used this model to derive the transient reflectivity induced by a fast Nd pulse for the 10.6 and 119μ radiation. The fit allowed us to derive a new valuation of both the γ_2 and γ_3 coefficients in InSb.

The transient reflectivity can be derived from the complex dielectric constant ε of the material, which depends on the free-carrier distribution N according to the Drude theory [8]

$$\varepsilon(x, t) = \varepsilon_L - \frac{\omega_e^2 \tau_e^2}{(1 + \omega_p^2 \tau_e^2)} \left(1 - i \frac{1}{\omega_p \tau_e} \right) - \frac{\omega_h^2 \tau_h^2}{(1 + \omega_p^2 \tau_h^2)} \left(1 - i \frac{1}{\omega_p \tau_h} \right) + i\beta(\omega_p)N(x, t) \quad (1a)$$

where

$$\omega_{e,h}^2 = \frac{N(x, t)q^2}{m_{e,h}\varepsilon_0}. \quad (1b)$$

$\omega_{e,h}$ are the plasma angular frequencies for e = electrons and h = holes, m_e and m_h being their relative effective mass, and τ_e , τ_h being the relative collision times. $N(x, t)$ is the carrier density distribution, assumed equal for e and h, and neglecting the effect of electrical polarization. ε_0 , ε_L are the dielectric constants in the vacuum and in the semiconductor respectively, q is the electron charge, ω_p is the angular frequency of the optical probe and $\beta(\omega_p)$ is the imaginary correction due to the carrier intraband absorption. We have posed $\beta(\omega_p) = 4 \times 10^{-18} \text{ cm}^{-3}$,

deriving it from the measured InSb absorption coefficient at $10\ \mu$ ($\sim 20\ \text{cm}^{-1}$) and the intrinsic concentration N_i .

The relaxation times $\tau_{e,h}$ can be derived from the relation (8)

$$\tau_{e,h} = \frac{\mu_{e,h} m_{e,h}}{q} \quad (1c)$$

where $\mu_{e,h}$ are the electron and hole mobility respectively. In equations (1) we have assumed that the plasma dynamic is planar and evolves along the semiconductor x axis normal to the incident surface, a condition quite correct for $\varepsilon_L \gg \varepsilon_0$ [10]. To calculate the exact optical response we need to sum the effect of several different semiconductor sub-layers because the $N(x, t)$ carrier distribution is generated in the pump absorption depth and relaxes with the semiconductor dynamics. The expression describing the whole dynamical process is [8]

$$\frac{\partial N(x, t)}{\partial t} - D \frac{\partial^2 N(x, t)}{\partial x^2} = G(x, t) - R(x, t) \quad (2)$$

where D is the ambipolar diffusion coefficient, G and R are the space–time dependent generation and recombination processes respectively. The ambipolar diffusion coefficient is not critical and it can be derived by the usual relations, and posed to $D = 20\ \text{cm}^2\ \text{s}^{-1}$ [2, 4].

By assuming for the pump pulse a Gaussian shape with an FWHM $2 \ln 2 \Delta$ time width, and E total energy absorbed on the area A , the expression for $G(x, t)$ becomes

$$G(x, t) \cong \frac{2\pi^{0.5} E}{A \Delta \alpha h \omega_p} \exp\left(-\frac{(t - xn/c)^2}{\Delta^2}\right) \exp(-\alpha x) \quad (3)$$

with n the diffraction index and α the absorption coefficient. The recombination processes are given by

$$R(x, t) = -\gamma_3 N^3(x, t) - \gamma_2 N^2(x, t) - \gamma_1 N(x, t) \quad (4)$$

where γ_3 is the ‘cubed’ AR, γ_2 is the radiative recombination plus the ‘squared’ AR and γ_1 is the impurity recombination plus the ‘linear’ AR ($3\gamma_3 N_i^2$). In InSb the radiative recombination and the impurity recombination could be neglected with respect to the ‘squared’ and ‘linear’ AR processes respectively.

In order to compute the dynamical probe transmission/reflection, we have to consider the semiconductor as a stratified stack of sublayers with different dielectric complex constants. By using the approach of [8] the overall reflectivity at the front surface and the sample transmission can be calculated in the time. Details are reported in [8].

The stratification approach involves also the interference effects. That means a fine space and time division and very long calculation time for thick samples.

It has been demonstrated in [10] that interference effects can be neglected for the Brewster incidence. The Brewster incidence also allows us to transfer the whole pump energy to the semiconductor.

2. Experimental results and discussion

We have measured the InSb $10.6\ \mu$ transient reflectivity near the Brewster angle with the apparatus described in [9] and [10] and briefly described here. The CO_2 laser emits 300 ns FWHM multimode pulses with a μs tail while Nd emits typically up to 40 mJ energy, 1.3 ns FWHM pulses at 0.5 Hz repetition rate. Both the beams are matched unfocused on a InSb intrinsic plate supplied by Wafer Technology Ltd. The CO_2 laser incidence is near the Brewster incidence and the residual 10 micron reflectivity allows us to calibrate the intensity of dynamical reflectivity. The reflected $10\ \mu$ beam is detected by using a fast Molelectron P5 pyroelectric and

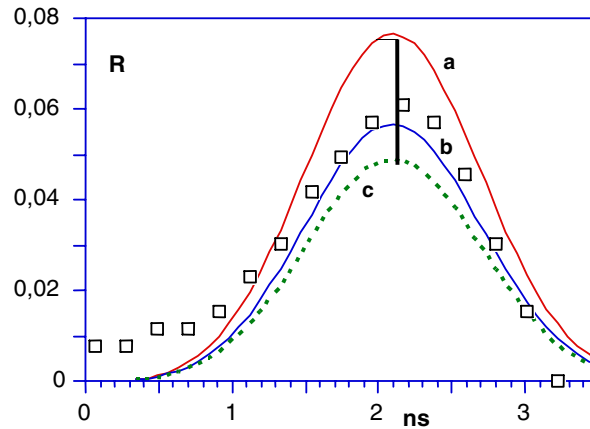


Figure 1. R = experimental reflectivity pulse against the time t at 10.6μ (squares) compared with some theoretical pulses: $a = \gamma_2 = 8 \times 10^{-9}$ and $\gamma_3 = 5 \times 10^{-26}$, $b = \gamma_2 = 8 \times 10^{-9}$ and $\gamma_3 = 8 \times 10^{-26}$, $c = \gamma_2 = 8 \times 10^{-9}$ and $\gamma_3 = 10 \times 10^{-26}$. The segment is the experimental error on the peak value.

the signals are recorded with a Tektronics digital oscilloscope with 500 MHz bandwidth. In order to eliminate the mode beat modulations, due to the CO_2 laser multimode emission, the observed reflected pulses are averaged over 90 shots.

Due to the fast AR in InSb, the 10μ FWHM reflected pulses have the same time behaviour as the driving Nd pulses, but the reflectivity peak is related to the recombination constants γ_2 and γ_3 and we can fit the experimental results by calculating the theoretical pulse. In the fit we have used the following constants: $m_e = 0.02m_0$ and $m_h = 0.45m_0$ [11] where m_0 is the free electron mass, and the mobility $\mu_e = 78000 \text{ cm}^2 \text{ V}^{-1} \text{ s}^{-1}$ and $\mu_h = 750 \text{ cm}^2 \text{ V}^{-1} \text{ s}^{-1}$ [12]. We have also considered that the mobility and diffusivity can be reduced at large plasma densities, so we have introduced for these quantities an heuristic correction functions fitted to the data reported in [13]. Other constants used in the fit are $E/A = 7 \text{ mJ cm}^{-2}$, $\Delta = 0.7 \text{ ns}$ and $\alpha = 5 \times 10^4 \text{ cm}^{-1}$ [12]. In the ns scale of our experiment the γ_1 ‘linear’ recombination is totally negligible; in any case we have posed $\gamma_1 = 8 \times 10^7 \text{ s}^{-1}$ the ‘linear’ AR coefficient for $\gamma_3 \sim 1 \times 10^{-25}$, that is the typical recombination rate of InSb undoped photodiodes [5].

In figure 1 we report the experimental pulsewidth compared with some theoretical pulses by varying γ_3 . In fact we have observed that the fit is insensitive to the γ_2 choice and it was necessary to consider the ‘cubed’ AR process. For this reason we have fixed $\gamma_2 = 8 \times 10^{-9} \text{ cm}^{-3} \text{ s}^{-1}$ as the mean value from [1, 2, 5]. From the fits we derive $\gamma_3 = 7.5 \pm 2.5 \times 10^{-26}$, where the error is mainly related to the valuation of the reflectivity peak. The obtained γ_3 value is inversely dependent on the m_e choice. For example by using $m_e = 0.013$ [12] we derive $\gamma_3 = 13 \pm 3 \times 10^{-26}$. In contrast the fits are insensitive to a change of m_h and to the plasma mobility correction of [13].

Our γ_3 value is larger than other experimental estimations. To confirm our surprising result we have applied our model to the transient front reflectivity at 119μ induced by a 30 ps Nd pulse, in the experiment described in [14]. The pulse (square points) reported in figure 2 is derived from the reflectivity trace reported in figure 6 of [14]. With respect to the original trace the signal is inverted in sign and corrected by means of a linear subtraction of the slow thermal negative tail. This slow signal is due to the film heating that increases the N_i concentration and so reduces the reflectivity according to the Drude model, in fact, for front lighting, the minimum 119μ reflectivity is expected at 42°C [14]. The transient reflectivity shows further

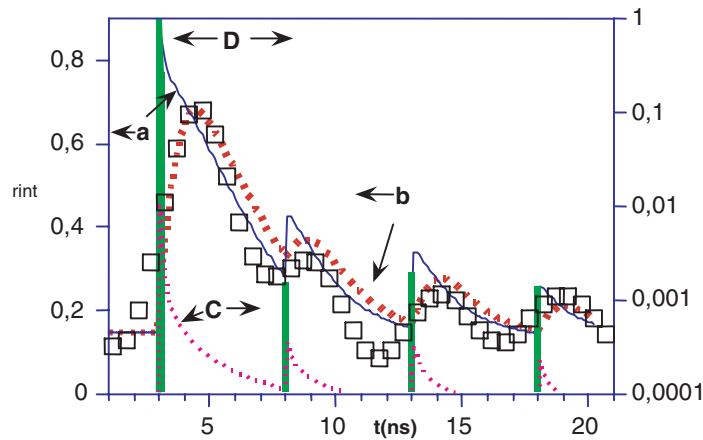


Figure 2. Fitting of a 119μ transient reflectivity R versus the time t (square points): curve a = real transient reflectivity, curve b = transient reflectivity convoluted to the detection time of the apparatus. Heavy vertical lines D are the ps Nd normalized pulses in the log scale and curve C is the plasma behaviour in the log scale normalized to $1.5 \times 10^{20} \text{ cm}^{-3}$ unit. Fit choice $\gamma_2 = 8 \times 10^{-9}$ and $\gamma_3 = 5 \times 10^{-26}$.

small peaks due to weak secondary Nd pulses at the cavity transit time delay, and its signal is convoluted by the electronic response time; both these effect must be considered in a fit.

A typical fit with the plasma-mobility correction is also reported in figure 2; the thin trace, a, is the real transient reflectivity, while the thick curve b is the time convoluted signal. The figure shows also, in a log scale, the Nd normalized power (D spikes) and the surface plasma density (curve c) normalized to the $1.5 \times 10^{20} \text{ cm}^{-3}$ unit. The fit shows that secondary peaks are produced by the very weak secondary Nd pulses and the tails of the FIR pulses are produced at weak plasma densities in the 1×10^{17} range. For these densities the mobility correction of [13] can be neglected. The figure 2 transient reflectivity was induced by an estimated 0.7 mJ cm^{-2} Nd fluence; besides, to compare the calculated pulses to the corrected experimental pulse we have introduced an electronic time response (1.1 ns) derived by fitting the left-hand side of the FIR pulses.

In figure 2 the effect of the AR recombination can be derived by fitting the descending side of the FIR pulses. In this region of weak plasma the reflectivity is sensitive to the γ_2 choice as shown in figure 3. From figure 3, by comparing different fittings we derive $\gamma_2 = 7 \pm 3 \times 10^{-9}$ and $\gamma_3 = 7 \pm 3 \times 10^{-26}$ in agreement with the 10μ fit obtained at much larger stationary plasma densities (2×10^{19}). In contrast to figure 1, the fits reported in figures 2 and 3 are quite insensitive to the m_e choice because the reflection peak is saturated near unity and the physical information is derived from the reflectivity recovery time.

It is evident from our fits that the γ_3 coefficient cannot be neglected and that our γ_2, γ_3 valuations are in agreement with the theoretical calculations reported in [2, 3, 5, 15], but they are two to three times larger than the theoretical calculations reported in [1] and [6]. That means that the effect of a dense plasma on the InSb band structure has been overrated in [1–4]. To explain their different conclusions we have to consider that in [1–4] the analysis has been performed with a simplified model of the plasma dynamics, directly relating the AR time to the recovery time of the transient signals.

To further confirm our results we have applied our model to the reflected and transmitted pulses reported in [4] and [16]. By using their estimated fluence (0.5 mJ cm^{-2} @ 6 ps pulsewidth) we have obtained a good fit by using the Auger constants derived in our

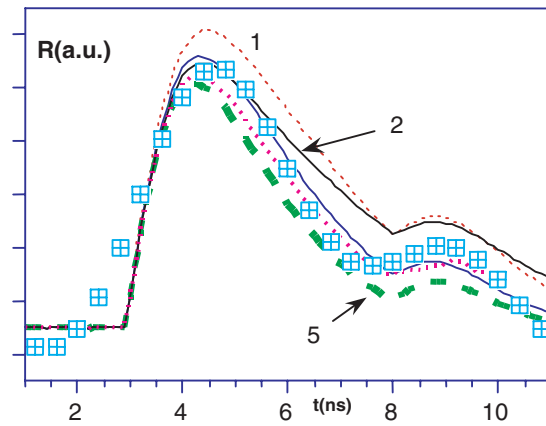


Figure 3. R = experimental reflectivity pulse against the time t at 119μ (squares) compared with some theoretical pulses at different choices. (1) $\gamma_2 = 10 \times 10^{-9}$, $\gamma_3 = 2 \times 10^{-26}$; (2) $\gamma_2 = 5 \times 10^{-9}$, $\gamma_3 = 10 \times 10^{-26}$; (3) $\gamma_2 = 10 \times 10^{-9}$, $\gamma_3 = 5 \times 10^{-26}$; (4) $\gamma_2 = 7.5 \times 10^{-9}$, $\gamma_3 = 10 \times 10^{-26}$; (5) $\gamma_2 = 10 \times 10^{-9}$, $\gamma_3 = 10 \times 10^{-26}$.

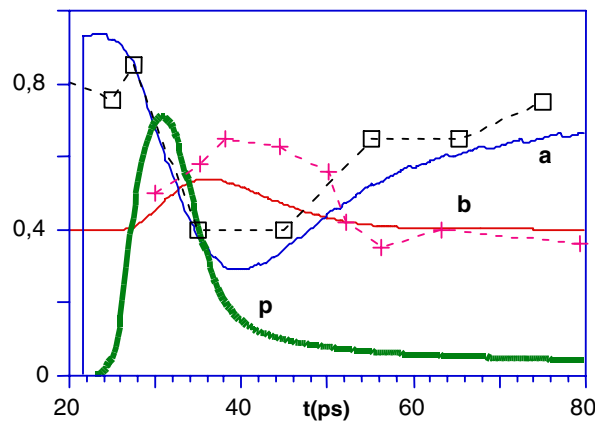


Figure 4. 10μ transient reflectivity R (crosses) and transmission T (squares) versus the time t reported in [4] and [13]. a = calculated transient transmission, b = calculated transient reflectivity for $\gamma_2 = 8 \times 10^{-9}$, $\gamma_3 = 5 \times 10^{-26}$, p = calculated surface plasma density in $1 \times 10^{-19} \text{ cm}^{-3}$ units.

measurements, as shown in figure 4. In this figure the transient reflectivity and transmission are convoluted with the 20 ps time of detection apparatus that matches the experimental reflectivity pulsewidth. Even in this case the mobility correction of [13] seems not to be influential. It is worth noting that the γ_3 coefficient used in the fit is a critical value; smaller values give a better fit of the reflection peak but do not reproduce the transmission pulse width. As in the fit of figure 1, the derived γ_3 coefficient is inversely dependent on the m_e value used in the fit.

The surface plasma density p also reported in figure 4 explains the error made in [16], where the 35 ps recovery time of the transmission dip was attributed to the nominal plasma density peak (1×10^{20}) while, 20 ps after the Nd pulse, the plasma is in the 1×10^{18} range and for this density value the 35 ps recovery time is equivalent to $\gamma_3 \sim 2 \times 10^{-25}$.

3. Conclusion

The dynamical IR–FIR reflectivity induced in InSb has been used to measure the constants of the AR process. By applying a complex dynamical model for a stack semiconductor structure with an induced transient distribution of photocarriers, the *a priori* approach allowed a more correct calculation of the Auger coefficients than in previous works and we have obtained values in better agreement with the theory. From our fits we derive the estimations $\gamma_3 = 7 \pm 3 \times 10^{-26} \text{ cm}^6 \text{ s}^{-1}$ and $\gamma_2 = 7 \pm 3 \times 10^{-9} \text{ cm}^3 \text{ s}^{-1}$. It is worth noting that by subtracting from γ_2 the ‘quadratic’ AR contribution $3\gamma_3 N_i$ we can derive a radiative recombination coefficient around $2 \times 10^{-9} \text{ cm}^3 \text{ s}^{-1}$ that is one order of magnitude larger than the result of [3], so that we have to suppose $\gamma_3 \sim 10 \times 10^{-26}$ for weak plasmas.

Acknowledgments

The authors are indebted to Mr S Bartalini for his skilful technical assistance. This work has been partially supported by the Progetto Finalizzato MADESS II of the Italian Research Council.

References

- [1] Chazapis V, Blom H A, Vodopyanov K L, Norman A G and Phillips C C 1995 *Phys. Rev. B* **52** 2516–21
- [2] Almazov L A, Liptuga A I, Malyutenko V K and Fedorenko L L 1980 *Sov. Phys.–Semicond.* **14** 1154–8
- [3] Bolgov S S and Fedorenko L L 1987 *Sov. Phys.–Semicond.* **21** 722–4
- [4] Fauchet P M 1982 *Phys. Status Solidi b* **110** K11–K15
- [5] Rogalsky A and Orman Z 1985 *Infrared Phys.* **25** 551–60
- [6] Beattie A R and White A M 1995 *J. Appl. Phys.* **79** 802–13
- [7] Ciesla C S *et al* 1996 *J. Appl. Phys.* **80** 2994–7
- [8] Vogel T, Dodel G, Holzhauser E, Salzmann H and Theurer A 1992 *Appl. Opt.* **31** 329–37
- [9] Marchetti S, Martinelli M, Simili R, Giorgi M and Fantoni R 2001 *Appl. Phys. B* **72** 927–30
- [10] Marchetti S, Martinelli M, Simili R, Giorgi M and Fantoni R *Phys. Scr.* at press
- [11] *Landolt–Bornstein New Series* 1987, Group III, vol 22, ed O Madelung (Berlin: Springer)
- [12] Kireev P 1975 *La Physique des Semiconducteurs* (Moscow: MIR)
- [13] Kruse P W 1970 *Semiconductors and Semimetals* vol 5, ed R K Willardson and A C Beer (New York: Academic)
- [14] Bertolini A, Carelli G, Ioli N, Massa C A, Moretti A, Ruffini A and Strumia F 2000 *J. Phys. D: Appl. Phys.* **33** 345–8
- [15] Beattie A R and Landsberg P T 1959 *Proc. R. Soc. A* **249** 16
- [16] Fauchet P M 1980 *Phys. Status Solidi a* **58** K211–14